EJN journal section:	Short communication
Word count (Introduction, methods, results and discussion)	3722
Abstract	250
Figures	4

Title:

***In vitro* evidence consistent with an interaction between wild type and a mutant SOD1 protein associated with canine degenerative myelopathy.**

Yao Qi[a], Paul Montague[b], Colin Loney[c], Clare Campbell[b], Intan N.F. Shafie[d], Thomas .J. Anderson[a] and Mark McLaughlin[a]*

[a] School of Veterinary Medicine, College of Medical, Veterinary and Life Science, University of Glasgow, Scotland, UK[b] Institute of Infection, Immunity and Inflammation, College of Medical, Veterinary and Life Science (MVLS), University of Glasgow, UK. [c] MRC, Centre for Virus Research, MVLS, University of Glasgow, UK. [d] Department of Veterinary Clinical Studies, Faculty of Veterinary Medicine, University Putra Malaysia Serdang, Malaysia.

*Corresponding Author: Dr Mark McLaughlin, Mark.McLaughlin@glasgow.ac.uk

Running Title:

Fluorescent tagged SOD1 mutant protein interaction and canine degenerative myelopathy

Key words

Canine; fALS; superoxide dismutase; aggregates; cell toxicity.

Abbreviations

DM (Canine degenerative myelopathy), fALS (familial amyotrophic lateral sclerosis), SOD1 (Cu/Zn superoxide dismutase), NBT (nitroblue tetrazolium), pWT-EGFP (plasmid with wild type SOD1-EGFP construct), pDM-EGFP (plasmid with DM SOD1-EGFP construct), pWT-cherry (plasmid with wild type SOD1-cherry construct), pDM-cherry (plasmid with DM SOD1-cherry construct).

Data Availability Statement

The data on which this paper is based have been deposited in Enlighten: Research Data http://dx.doi.org/10.5525/gla.researchdata.786.

Abstract

Canine degenerative myelopathy (DM) is a progressive neurological disorder that maybe considered to be a large animal model for specific forms of the fatal human disease, familial Amytrophic Lateral Sclerosis (fALS). DM is associated with a c118G>A mutation of the superoxide dismutase 1 (*Sod*1) gene and a significant proportion of cases are inherited in an autosomal recessive manner in contrast to the largely, but not exclusively, dominant mode of inheritance in fALS. The consensus view is that these *Sod*1/*SOD*1 mutations results in a toxic gain of function but the mechanisms remain unclear. Here we used an *in vitro* neuroblastoma cell line transfection system to monitor wild type and mutant forms of SOD1 fusion proteins containing either a Cherry or an enhanced green fluorescent protein (EGFP) tag. These fusion proteins retained SOD1 enzymatic activity on a native gel assay system. We demonstrate that SOD1 aggregate density is significantly higher in DM transfectants compared to wild type and show by co-immunoprecipitation and confocal microscopy, evidence for a potential interaction between wild type and mutant forms of SOD1 in co-transfected cells. While *in vitro* studies have shown SOD1 heterodimer formation in fALS models, this is the first report for DM SOD1. Therefore, despite for the majority of cases there is a difference in the mode of inheritance between fALS and DM, a similar interaction between wild type and mutant SOD1 forms can occur. Clarifying the role of SOD1 in DM may also be of benefit to understanding the role of SOD1 in fALS.

Introduction

Canine degenerative myelopathy (DM) is a progressive neurological disorder of the CNS that develops in aged dogs causing paresis of pelvic limbs that can progress to tetraplegia and ultimately death. The neurological signs are consistent with an upper motor neuron disease although there are lower motor neuron signs when euthanasia has been delayed (Griffiths and Duncan, 1975; Shelton et al., 2012). Although initially reported to affect mainly German Shepherd dogs (Averill, Jr., 1973; Griffiths and Duncan, 1975; Johnston et al., 2000), a range of small and large breeds have now been confirmed that develop the disease (Awano et al., 2009; Wininger et al., 2011; Zeng et al., 2014). The disease progression is rapid and ultimately results in euthanasia which is often elected when dogs reach a paraplegic state (Coates and Wininger, 2010; Griffiths and Duncan, 1975). The pathology of DM is characterised by an axonopathy and secondary myelin loss in the lateral columns of the ventral faniculi of the spinal cord, primarily within the thoracic/lumber intumescences (Johnston et al., 2000). Gliosis is widespread in the spinal cord (Johnston et al., 2000), and there are reports of neuronal and synaptic loss affecting both somatic sensory and motor tracts (Ogawa et al., 2014).

Diagnosis of DM in the clinic is achieved by exclusion of a wide range of common spinal cord diseases although a strong association has been found in cases that harbour a point mutation of the *Sod*1 gene (c118G>A) resulting in a predicted E40K amino acid substitution (Awano et al., 2009; Shafie et al., 2014; Zeng et al., 2014). The inheritance appears to be primarily autosomal recessive with Awano reporting on 100 cases across five breeds that 96% homozygotes (A/A) in DM diagnosed dogs although 34% (n=437) of the control group were also homozygotes (Awano et al., 2009). A similar pattern was reported in a more expansive study that confirmed eight DM cases were heterozygotes (A/G) (Zeng et al., 2014). An unbiased analysis by assessing dogs at a presymptomatic age (<6 years) then at a later age (>10 years) found that the incidence of these cases presenting clinical signs were 60% A/A, 4% G/A and 6% G/G suggesting characteristics of variable penetrance

(Zeng et al., 2014). Interestingly, another *Sod*1 gene mutation (c52A>T) has been reported which, to date, is only associated with the Bernese Mountain dog breed (Wininger et al., 2011). In addition, only a limited number of Bernese Mountain dogs were genotyped as heterozygotes for both c52A>T and c118G>A mutations and confirmed as DM cases by histopathology examination. This raises the possibility that compound heterozygotes may be a risk of developing DM (Pfahler et al., 2014; Wininger et al., 2011; Zeng et al., 2014). A potential modifier gene *Sp*110 has been reported that may influence the incidence of penetrance and possibly the age of onset (Ivansson et al., 2016).

The association between mutation(s) of the *Sod*1 gene together with the clinical features of DM has led to a proposal that DM may represent a natural and valid large animal model for specific forms of fALS. In fALS, an association with a mutation in the *SOD*1 gene occurs in approximately 20% of cases (Bunton-Stasyshyn et al., 2015) and up to 190 mutations have now been identified with an a seemingly unbiased distribution across the protein. To date there are no reports of a human *SOD*1 mutation that is equivalent to the DM c118G>A. However, disease penetrance rates in fALS associated with a *SOD*1 gene mutation is also complex; most are primarily inherited in a dominant mode although there are cases of recessive inheritance in fALS due to compound heterozygosity (Hand et al., 2001; Pasinelli and Brown, 2006) and also homozygote pedigrees of the D90A *SOD*1 mutation (Andersen et al., 1995).

As with the spectrum of *SOD*1 mutations in fALS, the causative relationship between the *Sod*1 mutation and the development of DM is currently unknown. It is generally agreed that in fALS and DM there is a toxic gain of function rather than a loss of function (Reaume et al., 1996) although a specific mechanism or indeed mechanisms common to the range of SOD1 mutants has not been identified. A number of transfection based studies have established that DM SOD1 can form aggregates in the cytoplasm of cultured cells including the embryonic kidney HEK293A and the neuroblastoma NSC34 cell lines with subsequent altered detergent solubility properties (Crisp et al., 2013; Nakamae et al., 2015). Similar alterations in conformation and a propensity to form

aggregates have also been observed in a number of fALS *SOD*1 mutations (Orrell, 2000; Pickles and Vande, 2012; Prudencio et al., 2009b; Rakhit and Chakrabartty, 2006). A recent study has described SOD1 aggregate accumulation in neurons and astrocytes of affected dogs suggesting a non-cell-autonomous process in DM (Kobatake et al., 2017). There are common degradation mechanisms for mutant SOD1 in DM and fALS, for example perturbation of the proteasome pathway (Nakamae et al., 2015). However, an intriguing and fundamental difference between DM and fALS is the high frequency of recessive cases in DM compared to high incidence of dominant inheritance in fALS (Nardone et al., 2016). WT and mutant SOD1 complexes can arise in fALS that appear to have a reduced propensity to form aggregates (Prudencio et al., 2009a; Weydert and Cullen, 2010; Witan et al., 2008; Witan et al., 2009) although soluble forms of SOD1, including heterodimers and trimeric complexes, may actually be more toxic than large SOD1 aggregates (Brotherton et al., 2013; Weichert et al., 2014; Zhu et al., 2018; Proctor et al., 2016). In asymptomatic and symptomatic heterozygous dogs, SOD1 aggregates have been observed (Awano et al., 2009; Nakamae et al., 2015). It is unclear if these aggregates contain homodimeric or heterodimeric complexes and if they have a functional relevance to disease development.

Here, the expression of a panel of WT and DM *Sod*1 cDNA constructs was used to track the distribution of fluorescent fusion SOD1 proteins in transiently transfected neuroblastoma cells. This confirmed that an increase in aggregate accumulation occurs in DM-SOD1 transfected cells compared to WT SOD1 transfectants. Furthermore, we present a combination of co-immunoprecipitation (IP) and confocal microscopy evidence that is consistent with a protein:protein interaction between the WT and mutant forms of SOD1 in cellular aggregates. These novel findings suggest the c118G>A *Sod*1 mutation alters some of the biochemical properties of SOD1 probably associated with the accumulation of aggregates.

Materials and Methods

Construction of Sod1 recombinants

Total cellular RNA was prepared from WT and DM T12 spinal cords using RNABee (Amsbio, UK) according to manufacturer's protocol. Random hexamer (Life Technologies, UK) primed cDNA synthesis was performed on 2 µg of RNA using SuperScript III following supplier's guidelines. Both WT and DM *Sod*1 cDNAs were subcloned into each of the amino fluorescent reporter vectors pEGFP-C3 and pCherry-C1 to generate (pWT-EGFP and pDM-EGFP) and (pWT-Cherry and pDM-Cherry). Two pairs of restriction enzyme site (in bold typeface) anchored PCR primers : (Fw *Xho*I 5/-**CTC GAG** ATG GAG ATG AAG GCC GTG TGC GTG-3/)/(Rv -*Hin*dIII 5/-**AAG CTT** TTA TTG GGC GAT CCC AAT GAC ACC – 3/.) and (Fw -*Xho*I 5/-**CTC GAG** ATG GAG ATG AAG GCC GTG TGC GTG-3/)/(Rv: *Bam*HI 5/-**GGA TCC** TTA TTG GGC GAT CCC AAT GAC ACC-3/) were used to amplify the 462 bp WT and DM *Sod*1 cDNAs corresponding to the 154 amino acid open reading frame (ORF). Using standard molecular techniques, amplicons were synthesised using the high fidelity proofreading EasyA Polymerase (Stratagene, USA) and cloned into the T/A vector pSC-A (Stratagene, USA). The inserts were released from the pSC-A recombinants by appropriate restriction enzyme digestion and covalently linked in-frame into at the corresponding sites in the multiple cloning site of the fluorescent tagged expression vectors pEGFP-C3 and pCherry-C1.

Cell culture

The SK-N-SH human neuroblastoma cell line (Helson et al., 1975) was used in this study. The cell line was maintained at 37 ^{0}C, 5 % CO_2 in DMEM high glucose medium (Invitrogen, UK), 10 % fetal bovine serum (FBS, Gibco, UK) and 1 % Penicillin-Streptomycin for a maximum of 20 passages.

Transfection, cell lysis and fluorescence microscopy

Cells were seeded on 13 mm Poly-L-Lysine treated coverslips in four-well plates at a cell density of $5x10^4$ per well or on six-well plates at $4x10^5$ per well and incubated overnight. Transfections were

performed using Lipofectamine® LTX with Plus™ Reagent (Invitrogen, UK) following manufacturer's recommendations and either fixed with 4 % paraformaldehyde (PFA) or harvested at the appropriate time point. The cells were visualised on a fluorescence microscope (IX70, Olympus, UK) and images captured using Image Pro Plus software (Media Cybernetics, USA). Nuclei were visualised in cells by treatment with 4',6-diamidino-2-phenylindole (DAPI, Sigma, UK). Cell counting was performed using Image J software. For each plasmid, three fields from four independent experiments were captured and the number of transfected cells with aggregates were quantified. For confocal microscopy, fluorescent samples were imaged using a 1.4NA Plan-Apochromat oil immersion objective lens fitted to a Zeiss LSM710 meta confocal microscope. The 405 nm laser line was utilised for DAPI, the 488 nm laser for green fluorescent protein (GFP) and the 561 nm laser for mCherry. Weighted co-localization coefficients were generated using Zen 2012 software (Zeiss, DE). All images have voxel sizes of 0.08 microns in each of x, y and z the number of confocal planes is one.

Cell lysates were prepared as described previously (McLaughlin et al., 2006), with a cell lysate buffer containing 1× TBS, 1 % Triton X-100, 1 mM EDTA, 1 mM Na Vanadate, 1 mM Na Pyrophosphate, and 1× Protease Inhibitor Cocktail (Invitrogen, UK). Cell lysates were mixed thoroughly by rotating at 4 °C for 30 minutes. Following centrifugation at 5,000 × g at 4 °C for 10 minutes, the supernatant and pellet fractions were collected and stored. The supernatant was assayed for protein content using the BCA assay system (Thermo scientific, UK) with bovine serum albumin as a reference standard.

SOD1 activity analysis using a native gel nitroblue tetrazolium (NBT) reduction assay system

SOD1 enzymatic activity was measured using a native gel NBT reduction system (Rakhit and Chakrabartty, 2006; Weydert and Cullen, 2010). This assay is based on the ability of SOD1 to retain its free radical savaging activity under native gel electrophoresis conditions thus inhibiting the reduction of tetrazolium to a blue complex generating white band(s) at the location of an active enzyme complex. Samples were mixed with a solution of glycerol and bromophenol blue and loaded onto a 10 % acrylamide native resolving gel with a 4 % stacking gel without SDS or dithiothreitol.

Gels were electrophoresed at 20 mA with chilled running buffer (25 mM Tris, 200 mM Glycine pH 8.3), stained with 1.23 mM NBT for 15 minutes then incubated with 28 mM TEMED and 280 mM riboflavin for 15 minutes in the dark. Following rinsing with MilliQ water, the gels were exposed to daylight and the colour reaction was allowed to develop over 5 to10 minutes.

Western blotting

Western blotting procedure was performed as described previously (McLaughlin et al., 2002). SDS PAGE was performed using NuPAGE®Novex® 4 – 12 % Bis-Tris Protein Gels, (Life Technologies, UK), the gel was transferred to nitrocellulose sheets using the iBlot® Transfer System, (Life Technologies, UK), blocked with 5 % non-fat milk powder in 1× Tris-buffered saline with Tween 20 (TTBS) and probed with the following primary antibodies anti-Cu/Zn SOD1 at 1/2000 dilution (AD1 SOD1-100, rabbit polyclonal from ENZO Life Science, USA), anti-GFP at 1/5000 (Abcam, UK, goat polyclonal Ab 6673), anti-Cherry at1/2000 (Abcam, UK, mouse monoclonal 125096) anti-β-Actin at 1/100,000 (Sigma Aldrich, UK mouse monoclonal clone AC-15, A-5441). Following several washes, nitrocellulose membranes were incubated with horseradish peroxidase-linked (HRP) secondary antibody in 5 % milk powder in TTBS and the immunocomplex detected by chemiluninescence ECL reaction (Thermo Fisher Scientific, UK). The signal intensity of the protein bands were quantified using Image J software (National Institute of Health, USA).

Immunoprecipitation

Rabbit polyclonal antibodies against GFP (Abcam ab290, 25 μg), Cherry (Abcam ab183628, 20 μg) and 10 μl of normal rabbit sera were coupled to 200 μl of settled beads of rmp Protein A Sepharose Fast Flow (GE healthcare, UK) as previously described (McLaughlin et al., 2002). In brief, Protein A beads were incubated with the appropriate antibody for two hours at 4 ^{o}C with rotation, washed three times with 100 mM sodium borate pH 9.2 and incubated with 200 mM dimethyl pimelimidate for one hour. Beads were then washed with 50 mM glycine pH 2.5 to remove unbound

immunoglobulins and resuspended in 1 ml of 50 mM Tris pH 8.0. The immunoprecipitation reactions were performed by incubating 30 μg of cell lysate with 50 μl of antibody coupled beads in 500 μl volume of lysis buffer (10 mM Hepes, 120 mM $NaCl_2$, 1 % triton-X-100 containing protease and phosphatase inhibitors) with rotation over night at 4 ^{0}C. The beads were pelleted by centrifugation, washed with lysis buffer and re-suspended in 1 ml of 10 mM tris pH 8.0. Each sample was split into two aliquots, centrifuged and the immunocomplex denatured for SDS-PAGE analysis. Each aliquot was processed by Western blotting using a goat anti GFP at 1/3,000 (Abcam ab6673) and mouse monoclonal anti-Cherry antibody at 1/1,000 dilutions (Abcam ab125096). Each gel also had 1.5 μg of the appropriate cell lysate as a positive control.

Statistical analysis

All statistical analyses and graphs in this study were analysed by using GraphPad Prism 5.0 (GraphPad Software, USA). Where data sets had equal variance, statistical analysis was performed using a two tailed Student's t-test with confidence intervals of 95 % and the Welch t-test was employed where the variance between two data sets were unequal. Data are reported as mean±SEM, P value and F ratio.

Results

Characterisation of fluorescently tagged SOD1 fusion proteins

Transfected neuroblastoma cell line SK-N-SH lysates analysed by western blotting confirmed the recombinants were expressed in-frame (**Figure 1A)**. The anti-SOD1 antibody detected the endogenous SOD1 at ~20 kDa and the fusion proteins at the predicted molecular weight of ~48 kDa. This was determined with either anti-EGFP or anti-Cherry antibodies that detected the unconjugated EGFP or Cherry moieties at ~27 kDa and the fusion protein at ~48 kDa. The relative expression level was comparable between plasmids as indicted by the similar levels of β-actin.

Mean transfection rates from three independent experiments were 40.3±8%, 39.9±13.9%, 27.7±4.6% and 41.4±8% (mean±SEM) with SK-N-SH cells transfected with pWT-EGFP, pDM-EGFP, pWT-Cherry and pDM-Cherry respectively for 48 hours. As depicted in **Figure 1B,** similar to the empty vectors, the majority of SK-N-SH transfected cells expressing pWT-EGFP and pWT-Cherry displayed a uniform pattern of green and red fluorescence respectively in the cytoplasm. In contrast, a bright punctate cytoplasmic pattern (identified by arrows), possibly indicative of protein aggregates, was evident in a higher percentage of cells expressing DM cDNAs compared to WT constructs (16.7±2.0% of pDM-EGFP compared to 5.8±2.0% pWT-EGFP and 15.8±5.1 pDM-Cherry compared to 2.6±0.6% pWT-Cherry transfectants (mean±SEM) (**Figure 1C**). The difference in the density of-aggregate containing cells was statistically significant (p=0.0086 for pWT-EGFP versus pDM-EGFP (Students t-test, F ratio of 1.02) and p= 0.0145 for pWT-Cherry versus pDM-Cherry (Welch t-test, since F ratio =18.5, P=0.03 confirming unequal variance between data sets).

SOD1 enzymatic activity of the fusion proteins was analysed using the native gel NBT system (**Figure 2A**) where SOD1 scavenging activity can be visualised on the gel. Two prominent bands of activity were observed in non-transfected cells that may represent both copper/zinc SOD and manganese SOD (indicated with black arrowheads). Several additional activity bands were observed with pWT-

EGFP (Lane 2) and pDM-EGFP (Lane 3) (indicated by the green arrows) and in pWT-Cherry (Lane 5) and pDM-Cherry transfectants (Lane 6) (indicated with the red arrows). The signal intensity with pDM-Cherry was routinely lower compared to the other *Sod*1 fusion constructs and tended to fade during the reaction process. Analysis of lysates prepared from co-transfected cells (pWT-EGFP/pDM-Cherry) (Lane 4) and (pDM-EGFP/pWT-Cherry) (Lane 7), also showed additional bands compared to the non-transfected cells (Lane 1). The banding profile observed with the NBT system is consistent with the fusion proteins retaining SOD1 enzymatic activity and is in agreement with reports on the activities of human *SOD*1 constructs using this method (Weichert et al., 2014; Weydert and Cullen, 2010; Witan et al., 2009). The variability between the WT and DM SOD1 banding patterns may indicate changes in the composition of proteins associated with SOD1 under native gel conditions. Western blotting analysis (**Figure 2B**) confirmed the presence of the different SOD1-fusion proteins in these lysates.

Co-expression of WT and mutant Sod1 cDNAs in transfected cells

SK-N-SH cells were co-transfected (**Figure 3**) with combinations of pWT-EGFP/pDM-Cherry (Panels 1 and 2) and pWT-Cherry/pDM-EGFP for 48 hrs (Panels 3 and 4) and analysed for protein co-localisation by confocal microscopy**.** Aggregates corresponding to bright fluorescent punctuate spots were detected in the green channel (WT-EGFP Panel 1, and DM-EGFP Panel 3) and also in the red channel (DM-Cherry Panel 1, and WT-Cherry Panel 3). These intense areas of fluorescence were unevenly distributed in the cytoplasm surrounding the nucleus. The merged images displayed areas of punctate yellow fluorescence (Panels 1 and 3) suggests a co-localisation of the SOD1 fusion proteins in the aggregates. A representative example of a transfected cell with no apparent aggregate formation is shown (Panels 2 and 4) where the yellow fluorescence pattern is more diffuse throughout the cell. However, small punctate red spots can be observed with DM-Cherry (white arrow in Panel 2) and green punctate (white arrow in Panel 4) with DM-EGFP that may represent early stages of SOD1 aggregate formation.

Immunoprecipitation (IP) pull down assay experiments (**Figure 4**) were performed to corroborate the confocal microscopy data. IPs were performed on cells co-transfected with (pWT-EGFP /pDM-Cherry) and the reciprocal (pWT-Cherry /pDM-EGFP) pairings using either anti-GFP or anti-Cherry antibodies were probed for the presence of GFP or Cherry fusion proteins. **Figure 4A** demonstrates that anti-Cherry IP also pulls down GFP-SOD1 protein, and **Figure 4B** shows that anti GFP IP also pulls down Cherry-SOD1 protein. The recovery of either WT-Cherry-SOD1 or DM-Cherry-SOD1 proteins appears to be more efficient using the anti-GFP antibody compared to the recovery of WT-GFP-SOD1 or DM-GFP-SOD1 with the anti-Cherry antibody. Normal rabbit serum failed to pull down either GFP or Cherry proteins. These co-precipitation experiments are consistent with a direct interaction between WT-GFP-SOD1 and DM-Cherry-SOD1 fusion proteins and between WT-Cherry and DM-EGFP-SOD1 fusion proteins.

Discussion

The formation of SOD1 aggregates in DM is a pathological feature of the homozygote spinal cord (Awano et al., 2009; Nakamae et al., 2015) compared to a much lesser extent in heterozygotes although the staining intensity reported in heterozygotes appears to be variable (Awano et al., 2009; Nakamae et al., 2015). Aggregate formation has been described in both neurons and astrocytes from homozygotes and a recent study using a DM-SOD1 specific antibody demonstrated that SOD1 aggregate formation (Awano et al., 2009; Kobatake et al., 2017; Nakamae et al., 2015; Ogawa et al., 2011) is restricted to heterozygote astrocytes (Kobatake et al., 2017). *In vitro* studies of aggregate formation and WT:mutant SOD1 interactions described in this study suggest that aggregates in the heterozygous scenario may be composed of both WT and mutant SOD1, possibly as protein dimers.

Although valuable information has been obtained from the use of fluorescent tagged constructs in fALS studies (Weichert et al., 2014; Witan et al., 2008; Witan et al., 2009) and DM (Crisp et al., 2013; Nakamae et al., 2015), the presence of a relative large protein tag may compromise some of the physiological properties of SOD1 (Stevens et al., 2010; Qualls et al., 2013). However, a recent study using a GFP based bicistronic expression system and a standard GFP fusion expression vector reported that both DM-SOD1 and the fusion protein GFP:DM-SOD1 form aggregates in SHSY5 neuroblastoma cells (Draper et al., 2016) suggesting the covalent linkage of a fluorescent tag does not significantly alter properties of the native SOD1. Using the native gel NBT system, we also show enzymatic activity of the SOD1 fusion proteins, albeit to a variable degree. The apparent difference in the WT-SOD1 and DM-SOD1 activity regions within the native gel raises the possibility that the DM-SOD1 protein form a distinct protein complex profile possibly involving chaperones such as the copper chaperone for SOD1 (CCS) that can influence the maturation of an active SOD1 complex (Banci et al., 2012).

Although there is variability in disease penetrance, an important and fundamental difference between DM and SOD1 associated fALS is the relatively high frequency of DM homozygotes

compared to the relatively high incidence of fALS heterozygotes. The fALS D90A *SOD*1 mutation is unusual in that both heterozygous and homozygous pedigrees have been reported and with variable penetrance for both (Andersen et al., 1995). Our data strongly suggests some degree of WT:mutant SOD1 heterodimeric interaction in neuroblastoma co-transfectants, which subsequently form aggregates. Since aggregates are found in both neurones and astrocytes in DM homozygotes but apparently only present in heterozygous astrocytes (Kobatake et al., 2017), this suggests that the cellular environment, possibly related to protein clearance pathways may influences the fate of the various forms of the SOD1 complexes.

Studies from fALS *in vitro* models have shown that wild type SOD1 can influence the folding and stability of mutant SOD1, possibly through heterodimer formation (Weichert et al., 2014; Witan et al., 2008). Furthermore, the co-expression of WT and mutant *SOD*1 constructs in transgenic models of fALS also results in a more severe phenotype with an earlier onset (Prudencio et al., 2010; Wang et al., 2009; Xu et al., 2015). The significance of SOD1 aggregates in heterozygote dogs in relation to the low incidence of DM in heterozygotes remains unknown.

In conclusion, the main observation from this study is that DM and wild type SOD1 can interact and possibly form heterodimers. While such an interaction has been described for some fALS associated SOD1 mutants, this is the first report for the DM associated mutant and wild type SOD1 protein interaction. DM is a naturally occurring large animal neurological condition and a potential model of fALS, although in contrast to fALS penetrance is high in mutant SOD1 homozygotes compared to heterozygotes. It could be speculated that this interaction influences SOD1 complex stability, toxicity and ultimately (depending on genetic background) disease penetrance. Extending our understanding of these properties and their impact on disease progression will be important given the therapeutic potential of anti SOD1 strategies for treating fALS (Gertsman et al., 2019; Iannitti et al., 2018) and DM.

Figure 1. Confirmation of the presence of SOD1 fusion proteins in SK-N-SH transfectants.

(A) Western blot analysis of lysates from SK-N-SH cells transfected with pEGFP, pWT-EGFP and pDM-EGFP (left hand panel) and pCherry, pWT-Cherry and pDM-Cherry (right hand panel) for 48 hours confirmed the presence of GFP and Cherry SOD1 fusion proteins at ~49 kDa, GFP and Cherry proteins at ~27 kDa in cells transfected with the empty vectors and endogenous SOD1 at ~20 kDa. Images captured by fluorescent microscopy (B) show a predominantly cytoplasmic distribution of fluorescence in pEGFP and pCherry transfectants. A representative example WT SOD1 fusion protein transfected cells lacking aggregates and DM-SOD1 fusion protein transfected cells with aggregates is shown (arrows).

The density of cells that display aggregates was quantified (C) in a defined area at 20x magnification from four independent experiments. The difference in the density of-aggregate containing cells was statistically significant ($p=0.0086$ for pWT-EGFP versus pDM-EGFP (Students t-test, F ratio of 1.02) and $p= 0.0145$ for pWT-Cherry versus pDM-Cherry (Welch t-test, since F ratio =18.5, $P=0.03$ confirming unequal variance between data sets).

Figure 2. Analysis of SOD1 enzymatic activity by native gel electrophoresis.

Cell lysates were analysed for SOD1 activity (A) and for the presence of fusion proteins (B). The various transfection treatments were:- Non-transfected SK-N-SH cells (Lane 1), cells transfected with pWT-EGFP (Lane 2), pDM-EGFP (Lane 3), pWT-EGFP and pDM-Cherry (Lane 4), pWT-Cherry (Lane 5), pDM-Cherry (Lane 6) and pWT-Cherry and pDM-EGFP (Lane 7). Endogenous SOD1 activity (A) is indicated by the black arrows and present in all lanes. Additional bands were identified in cells expressing the EGFP recombinants (green arrows) and Cherry recombinants (red arrows). The banding pattern appeared to differ between the WT and DM-SOD1 fusion proteins (compare Lanes 2 and 3). The enzymatic activity of the mutant SOD1-Cherry protein (A, Lane 6) was weak compared to the other constructs. (B) Western blots of the same cell lysates confirmed the presence of SOD1

fusion proteins. The upper panel in B demonstrates the presence of endogenous SOD1 (Lanes 1-7) and SOD1 fusion proteins (Lanes 2-7). The presence of the appropriate fluorescent tag was confirmed for GFP (B, middle panel, Lanes 2, 3, 4 and 7) and Cherry (B, lower panel, Lanes 4-7).

Figure 3. Confocal microscopy analysis of cells co-expressing wild type and mutant cDNAs.

Representitive confocal images of SK-N-SH cells co-transfected with pWT-EGFP /pDM-Cherry (Panels 1 and 2) and pWT-Cherry /pDM-EGFP (Panels 3 and 4) depict the presence and absence of aggregates . The nuclei for each example is stained with DAPI. The merged images displayed areas of punctate yellow fluorescence (Panels 1 and 3) suggesting a co-localisation in the aggregates. A representative example of a transfected cell shows no apparent aggregates (Panels 2 and 4) where the yellow fluorescence pattern is more diffuse throughout the cell. Small punctuate red spots (arrow) can be observed with pDM-Cherry (Panel 2) and green puncta (arrow) with pDM-EGFP (Panel 4) that may represent early stages of aggregate formation. (Scale bar=10 μm).

Figure 4. Co-immunoprecipitation of cells co-expressing wild type and mutant cDNAs.

Evidence for a protein : protein interaction between GFP and Cherry fusion proteins was assessed by co-immunoprecipitation. Lysates from co-transfectants (WT-EGFP/DM-Cherry, DM-EGFP/WT-Cherry) were immunoprecipitated with either anti-GFP or anti-Cherry then assessed by western blot with anti-GFP (A) or anti-Cherry (B). L indicates lysate (1.5ug, 5% of the amount used in the IP reaction), E depicts an empty lane, NRS depicts IP with normal rabbit sera, Cherry IP with anti-Cherry antibody and GFP-IP with anti-GFP antibody. The combination of transfected cells is shown above each panel. The immunoprecipitation of the GFP-SOD1 with anti-Cherry and Cherry SOD1 with anti-GFP is indicated by the arrows and is clearly visible. The recovery of either WT-Cherry or DM-Cherry SOD1 with an anti-GFP antibody appears to be more efficient compared to the recovery of WT-GFP or DM-GFP with the anti-Cherry antibody.

Acknowledgements

This work was funded by the Ronald Miller Scholarship, School of Veterinary Medicine, University of Glasgow.

Author Contribution

Yao QI performed the majority of the cell biology experiments described in this study and contributed to the preparation of the manuscript. Paul Montague was responsible for the design of the plasmid constructs, supervision of the molecular cloning and made a significant contribution to the preparation of the manuscript. Clare Campbell assisted in the quantification of the cells containing aggregates. Colin Loney conducted the confocal microscopy analysis. Intan N.F. Shafie genotyped the cases used as the source of WT and mutant *Sod*1 mRNA and reviewed the manuscript. Thomas James Anderson was central to the design and supervision of the project and the preparation of the manuscript. Mark McLaughlin was the principal investigator who directed this project, supervised Yao Qi and Clare Campbell, performed NBT gel analysis, Western blotting and prepared the manuscript.

Disclosure Statement

There are no potential conflicts of interest for any of the authors of this manuscript. All authors have approved the final manuscript.

Reference List

Andersen,P.M., Nilsson,P., Ala-Hurula,V., Keranen,M.L., Tarvainen,I., Haltia,T., Nilsson,L., Binzer,M., Forsgren,L., and Marklund,S.L. (1995). Amyotrophic lateral sclerosis associated with homozygosity for an Asp90Ala mutation in CuZn-superoxide dismutase. Nat. Genet. *10*, 61-66.

Averill,D.R., Jr. (1973). Degenerative myelopathy in the aging German Shepherd dog: clinical and pathologic findings. J. Am. Vet. Med. Assoc. *162*, 1045-1051.

Awano,T., Johnson,G.S., Wade,C.M., Katz,M.L., Johnson,G.C., Taylor,J.F., Perloski,M., Biagi,T., Baranowska,I., Long,S., March,P.A., Olby,N.J., Shelton,G.D., Khan,S., O'Brien,D.P., Lindblad-Toh,K., and Coates,J.R. (2009). Genome-wide association analysis reveals a SOD1 mutation in canine degenerative myelopathy that resembles amyotrophic lateral sclerosis. Proc. Natl. Acad. Sci. U. S. A *106*, 2794-2799.

Banci,L., Bertini,I., Cantini,F., Kozyreva,T., Massagni,C., Palumaa,P., Rubino,J.T., and Zovo,K. (2012). Human superoxide dismutase 1 (hSOD1) maturation through interaction with human copper chaperone for SOD1 (hCCS). Proc. Natl. Acad. Sci. U. S. A *109*, 13555-13560.

Brotherton,T.E., Li,Y., and Glass,J.D. (2013). Cellular toxicity of mutant SOD1 protein is linked to an easily soluble, non-aggregated form in vitro. Neurobiol. Dis. *49*, 49-56.

Bunton-Stasyshyn,R.K., Saccon,R.A., Fratta,P., and Fisher,E.M. (2015). SOD1 Function and Its Implications for Amyotrophic Lateral Sclerosis Pathology: New and Renascent Themes. Neuroscientist. *21*, 519-529.

Coates,J.R. and Wininger,F.A. (2010). Canine degenerative myelopathy. Vet. Clin. North Am. Small Anim Pract. *40*, 929-950.

Crisp,M.J., Beckett,J., Coates,J.R., and Miller,T.M. (2013). Canine degenerative myelopathy: biochemical characterization of superoxide dismutase 1 in the first naturally occurring non-human amyotrophic lateral sclerosis model. Exp. Neurol. *248*, 1-9.

Draper, Z., Windley, C., Maile, R. J., and Piercy, R. Species-specific differences in cellular aggregation and localisation of virally transduced mutant and normal canine and equine superoxide dismutase 1 (sod1) proteins. J.Vet.Intern.Med (Proc.29th Symposium ESCV-ECVN) 30[6], p1929-p1955. 2016.

Gertsman,I., Wuu,J., McAlonis-Downes,M., Ghassemian,M., Ling,K., Rigo,F., Bennett,F., Benatar,M., Miller,T.M., and Da,C.S. (2019). An endogenous peptide marker differentiates SOD1 stability and facilitates pharmacodynamic monitoring in SOD1 amyotrophic lateral sclerosis. JCI. Insight. *4*, e122768.

Griffiths,I.R. and Duncan,I.D. (1975). Chronic degenerative radiculomyelopathy in the dog. J. Small Anim Pract. *16*, 461-471.

Hand,C.K., Mayeux-Portas,V., Khoris,J., Briolotti,V., Clavelou,P., Camu,W., and Rouleau,G.A. (2001). Compound heterozygous D90A and D96N SOD1 mutations in a recessive amyotrophic lateral sclerosis family. Ann. Neurol. *49*, 267-271.

Helson,L., Das,S.K., and Hajdu,S.I. (1975). Human neuroblastoma in nude mice. Cancer Res. *35*, 2594-2599.

Iannitti,T., Scarrott,J.M., Likhite,S., Coldicott,I.R.P., Lewis,K.E., Heath,P.R., Higginbottom,A., Myszczynska,M.A., Milo,M., Hautbergue,G.M., Meyer,K., Kaspar,B.K., Ferraiuolo,L., Shaw,P.J., and Azzouz,M. (2018). Translating SOD1 Gene Silencing toward the Clinic: A Highly Efficacious, Off-Target-free, and Biomarker-Supported Strategy for fALS. Mol. Ther. Nucleic Acids *12*, 75-88.

Ivansson,E.L., Megquier,K., Kozyrev,S.V., Muren,E., Korberg,I.B., Swofford,R., Koltookian,M., Tonomura,N., Zeng,R., Kolicheski,A.L., Hansen,L., Katz,M.L., Johnson,G.C., Johnson,G.S., Coates,J.R., and Lindblad-Toh,K. (2016). Variants within the SP110 nuclear body protein modify risk of canine degenerative myelopathy. Proc. Natl. Acad. Sci. U. S. A *113*, E3091-E3100.

Johnston,P.E., Barrie,J.A., McCulloch,M.C., Anderson,T.J., and Griffiths,I.R. (2000). Central nervous system pathology in 25 dogs with chronic degenerative radiculomyelopathy. Vet. Rec. *146*, 629-633.

Kobatake,Y., Sakai,H., Tsukui,T., Yamato,O., Kohyama,M., Sasaki,J., Kato,S., Urushitani,M., Maeda,S., and Kamishina,H. (2017). Localization of a mutant SOD1 protein in E40K-heterozygous dogs: Implications for non-cell-autonomous pathogenesis of degenerative myelopathy. J. Neurol. Sci. *372*, 369-378.

McLaughlin,M., Barrie,J.A., Karim,S., Montague,P., Edgar,J.M., Kirkham,D., Thomson,C.E., and Griffiths,I.R. (2006). Processing of PLP in a model of Pelizaeus-Merzbacher disease/SPG2 due to the rumpshaker mutation. Glia *53*, 715-722.

McLaughlin,M., Hunter,D.J., Thomson,C.E., Yool,D., Kirkham,D., Freer,A.A., and Griffiths,I.R. (2002). Evidence for possible interactions between PLP and DM20 within the myelin sheath. Glia *39*, 31-36.

Nakamae,S., Kobatake,Y., Suzuki,R., Tsukui,T., Kato,S., Yamato,O., Sakai,H., Urushitani,M., Maeda,S., and Kamishina,H. (2015). Accumulation and aggregate formation of mutant superoxide dismutase 1 in canine degenerative myelopathy. Neuroscience *303*, 229-240.

Nardone,R., Holler,Y., Taylor,A.C., Lochner,P., Tezzon,F., Golaszewski,S., Brigo,F., and Trinka,E. (2016). Canine degenerative myelopathy: a model of human amyotrophic lateral sclerosis. Zoology. (Jena) *119*, 64-73.

Ogawa,M., Uchida,K., Park,E.S., Kamishina,H., Sasaki,J., Chang,H.S., Yamato,O., and Nakayama,H. (2011). Immunohistochemical observation of canine degenerative myelopathy in two Pembroke Welsh Corgi dogs. J. Vet. Med. Sci. *73*, 1275-1279.

Ogawa,M., Uchida,K., Yamato,O., Inaba,M., Uddin,M.M., and Nakayama,H. (2014). Neuronal loss and decreased GLT-1 expression observed in the spinal cord of Pembroke Welsh Corgi dogs with canine degenerative myelopathy. Vet. Pathol. *51*, 591-602.

Orrell,R.W. (2000). Amyotrophic lateral sclerosis: copper/zinc superoxide dismutase (SOD1) gene mutations. Neuromuscul. Disord. *10*, 63-68.

Pasinelli,P. and Brown,R.H. (2006). Molecular biology of amyotrophic lateral sclerosis: insights from genetics. Nat. Rev. Neurosci. *7*, 710-723.

Pfahler,S., Bachmann,N., Fechler,C., Lempp,C., Baumgartner,W., and Distl,O. (2014). Degenerative myelopathy in a SOD1 compound heterozygous Bernese mountain dog. Anim Genet. *45*, 309-310.

Pickles,S. and Vande,V.C. (2012). Misfolded SOD1 and ALS: zeroing in on mitochondria. Amyotroph. Lateral. Scler. *13*, 333-340.

Proctor,E.A., Fee,L., Tao,Y., Redler,R.L., Fay,J.M., Zhang,Y., Lv,Z., Mercer,I.P., Deshmukh,M., Lyubchenko,Y.L., and Dokholyan,N.V. (2016). Nonnative SOD1 trimer is toxic to motor neurons in a model of amyotrophic lateral sclerosis. Proc. Natl. Acad. Sci. U. S. A *113*, 614-619.

Prudencio,M., Durazo,A., Whitelegge,J.P., and Borchelt,D.R. (2009a). Modulation of mutant superoxide dismutase 1 aggregation by co-expression of wild-type enzyme. J. Neurochem. *108*, 1009-1018.

Prudencio,M., Durazo,A., Whitelegge,J.P., and Borchelt,D.R. (2010). An examination of wild-type SOD1 in modulating the toxicity and aggregation of ALS-associated mutant SOD1. Hum. Mol. Genet. *19*, 4774-4789.

Prudencio,M., Hart,P.J., Borchelt,D.R., and Andersen,P.M. (2009b). Variation in aggregation propensities among ALS-associated variants of SOD1: correlation to human disease. Hum. Mol. Genet. *18*, 3217-3226.

Qualls,D.A., Crosby,K., Brown,H., and Borchelt,D.R. (2013). An analysis of interactions between fluorescently-tagged mutant and wild-type SOD1 in intracellular inclusions. PLoS. One. *8*, e83981.

Rakhit,R. and Chakrabartty,A. (2006). Structure, folding, and misfolding of Cu,Zn superoxide dismutase in amyotrophic lateral sclerosis. Biochim. Biophys. Acta *1762*, 1025-1037.

Reaume,A.G., Elliott,J.L., Hoffman,E.K., Kowall,N.W., Ferrante,R.J., Siwek,D.F., Wilcox,H.M., Flood,D.G., Beal,M.F., Brown,R.H., Jr., Scott,R.W., and Snider,W.D. (1996). Motor neurons in Cu/Zn superoxide dismutase-deficient mice develop normally but exhibit enhanced cell death after axonal injury. Nat. Genet. *13*, 43-47.

Shafie,I.N., McLaughlin,M., Burchmore,R., Lim,M.A., Montague,P., Johnston,P.E., Penderis,J., and Anderson,T.J. (2014). The chaperone protein clusterin may serve as a cerebrospinal fluid biomarker for chronic spinal cord disorders in the dog. Cell Stress. Chaperones. *19*, 311-320.

Shelton,G.D., Johnson,G.C., O'Brien,D.P., Katz,M.L., Pesayco,J.P., Chang,B.J., Mizisin,A.P., and Coates,J.R. (2012). Degenerative myelopathy associated with a missense mutation in the superoxide dismutase 1 (SOD1) gene progresses to peripheral neuropathy in Pembroke Welsh corgis and boxers. J. Neurol. Sci. *318*, 55-64.

Stevens,J.C., Chia,R., Hendriks,W.T., Bros-Facer,V., van,M.J., Martin,J.E., Jackson,G.S., Greensmith,L., Schiavo,G., and Fisher,E.M. (2010). Modification of superoxide dismutase 1 (SOD1) properties by a GFP tag--implications for research into amyotrophic lateral sclerosis (ALS). PLoS. One. *5*, e9541.

Wang,L., Deng,H.X., Grisotti,G., Zhai,H., Siddique,T., and Roos,R.P. (2009). Wild-type SOD1 overexpression accelerates disease onset of a G85R SOD1 mouse. Hum. Mol. Genet. *18*, 1642-1651.

Weichert,A., Besemer,A.S., Liebl,M., Hellmann,N., Koziollek-Drechsler,I., Ip,P., Decker,H., Robertson,J., Chakrabartty,A., Behl,C., and Clement,A.M. (2014). Wild-type Cu/Zn superoxide dismutase stabilizes mutant variants by heterodimerization. Neurobiol. Dis. *62*, 479-488.

Weydert,C.J. and Cullen,J.J. (2010). Measurement of superoxide dismutase, catalase and glutathione peroxidase in cultured cells and tissue. Nat. Protoc. *5*, 51-66.

Wininger,F.A., Zeng,R., Johnson,G.S., Katz,M.L., Johnson,G.C., Bush,W.W., Jarboe,J.M., and Coates,J.R. (2011). Degenerative myelopathy in a Bernese Mountain Dog with a novel SOD1 missense mutation. J. Vet. Intern. Med. *25*, 1166-1170.

Witan,H., Gorlovoy,P., Kaya,A.M., Koziollek-Drechsler,I., Neumann,H., Behl,C., and Clement,A.M. (2009). Wild-type Cu/Zn superoxide dismutase (SOD1) does not facilitate, but impedes the formation of protein aggregates of amyotrophic lateral sclerosis causing mutant SOD1. Neurobiol. Dis. *36*, 331-342.

Witan,H., Kern,A., Koziollek-Drechsler,I., Wade,R., Behl,C., and Clement,A.M. (2008). Heterodimer formation of wild-type and amyotrophic lateral sclerosis-causing mutant Cu/Zn-superoxide dismutase induces toxicity independent of protein aggregation. Hum. Mol. Genet. *17*, 1373-1385.

Xu,G., Ayers,J.I., Roberts,B.L., Brown,H., Fromholt,S., Green,C., and Borchelt,D.R. (2015). Direct and indirect mechanisms for wild-type SOD1 to enhance the toxicity of mutant SOD1 in bigenic transgenic mice. Hum. Mol. Genet. *24*, 1019-1035.

Zeng,R., Coates,J.R., Johnson,G.C., Hansen,L., Awano,T., Kolicheski,A., Ivansson,E., Perloski,M., Lindblad-Toh,K., O'Brien,D.P., Guo,J., Katz,M.L., and Johnson,G.S. (2014). Breed distribution of SOD1 alleles previously associated with canine degenerative myelopathy. J. Vet. Intern. Med. *28*, 515-521.

Zhu,C., Beck,M.V., Griffith,J.D., Deshmukh,M., and Dokholyan,N.V. (2018). Large SOD1 aggregates, unlike trimeric SOD1, do not impact cell viability in a model of amyotrophic lateral sclerosis. Proc. Natl. Acad. Sci. U. S. A *115*, 4661-4665.

Figure 1

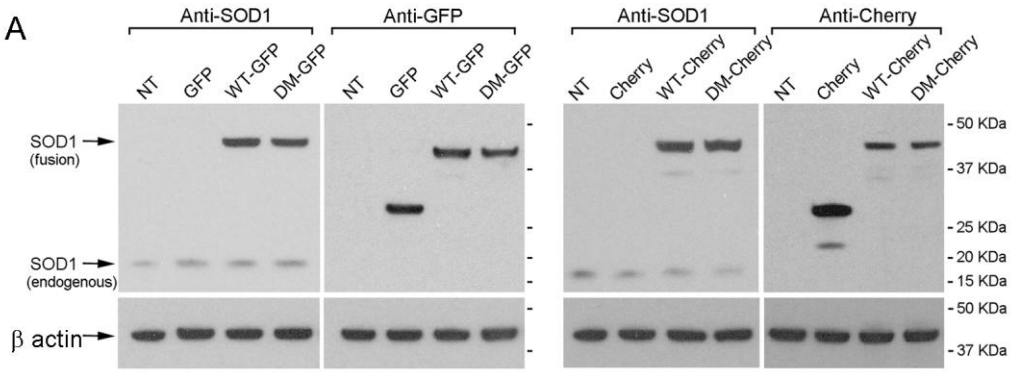
A
Anti-SOD1
Anti-GFP
Anti-SOD1
Anti-Cherry
NT
GFP
WT-GFP
DM-GFP
NT
GFP
WT-GFP
DM-GFP
NT
Cherry
WT-Cherry
DM-Cherry
NT
Cherry
WT-Cherry
DM-Cherry
SOD1 (fusion)
SOD1 (endogenous)
β actin
50 KDa
37 KDa
25 KDa
20 KDa
15 KDa
50 KDa
37 KDa

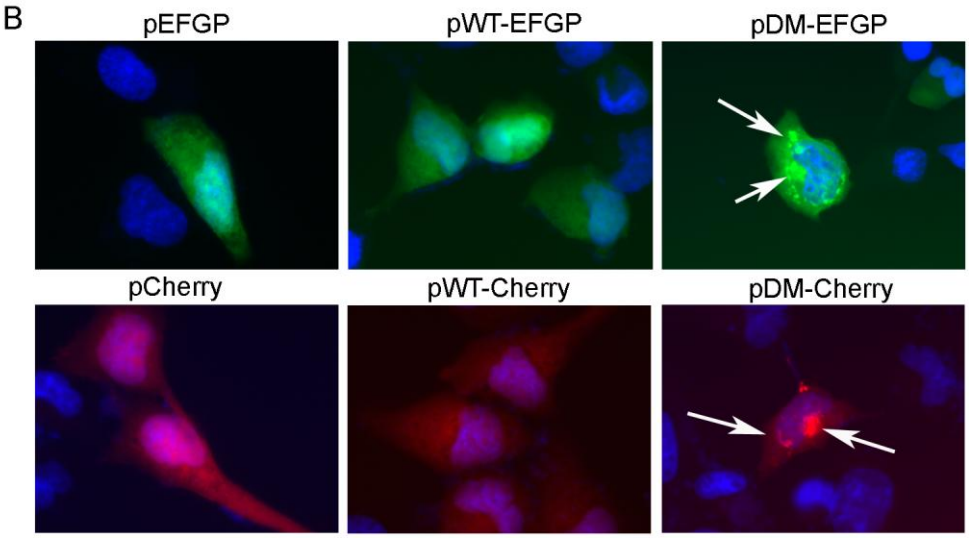
B
pEFGP
pWT-EFGP
pDM-EFGP
pCherry
pWT-Cherry
pDM-Cherry

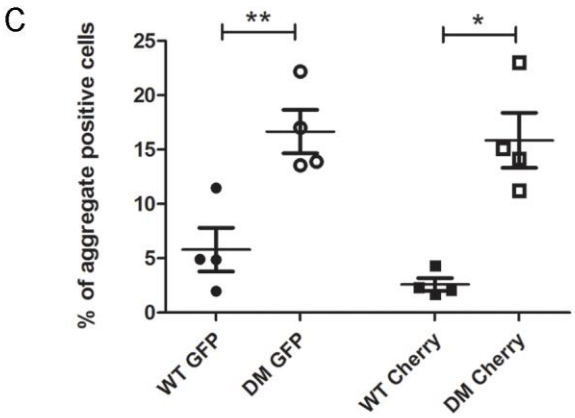
C
% of aggregate positive cells
25
20
15
10
5
0
**
*
WT GFP
DM GFP
WT Cherry
DM Cherry

Figure 2

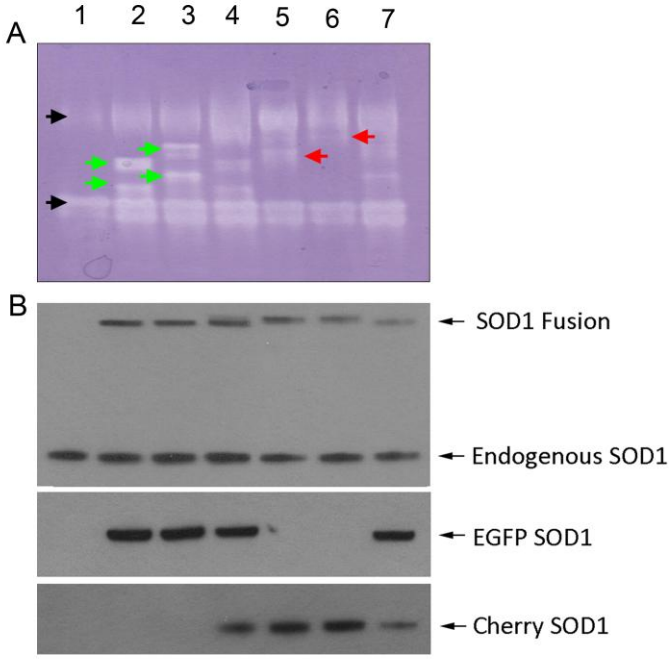
A
1 2 3 4 5 6 7
B
SOD1 Fusion
Endogenous SOD1
EGFP SOD1
Cherry SOD1

Figure 3

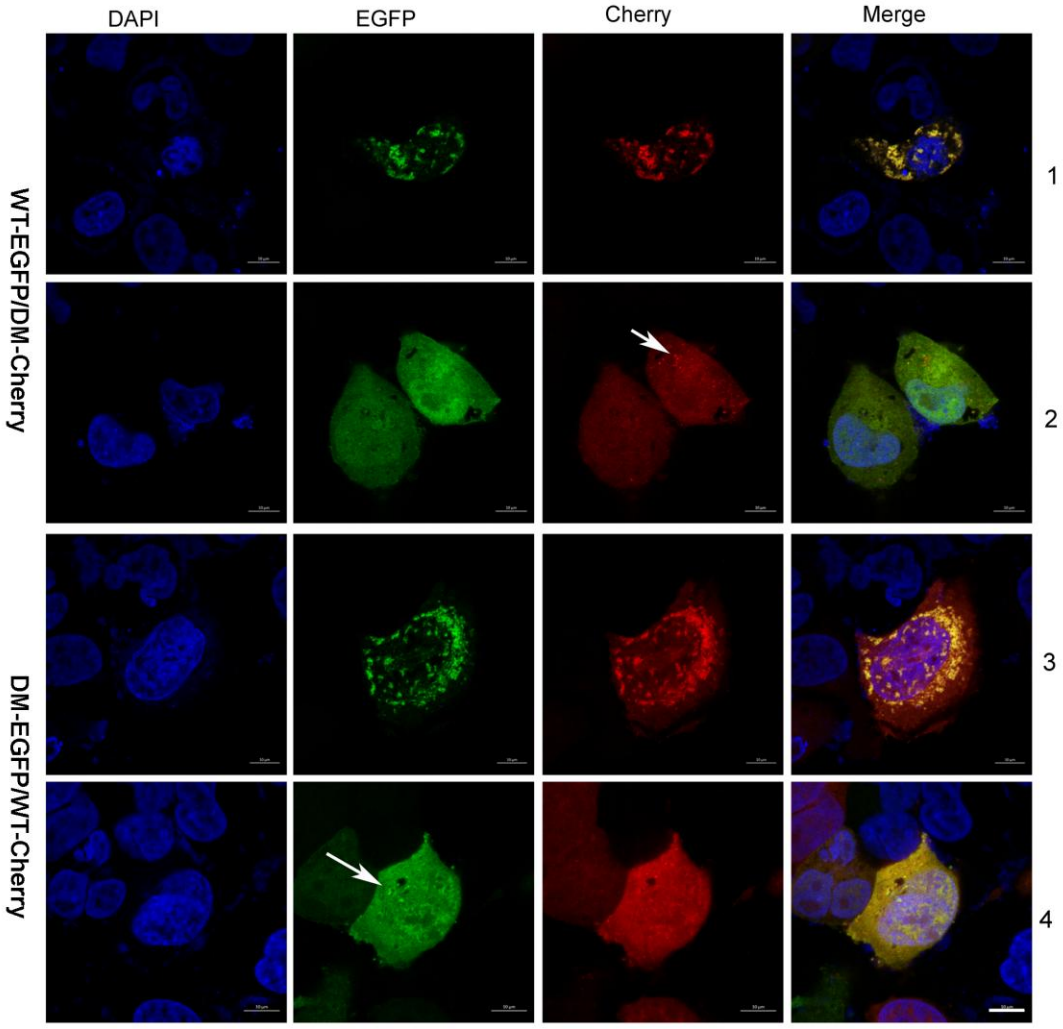
DAPI
EGFP
Cherry
Merge
WT-EGFP/DM-Cherry
DM-EGFP/WT-Cherry
1
2
3
4

Figure 4

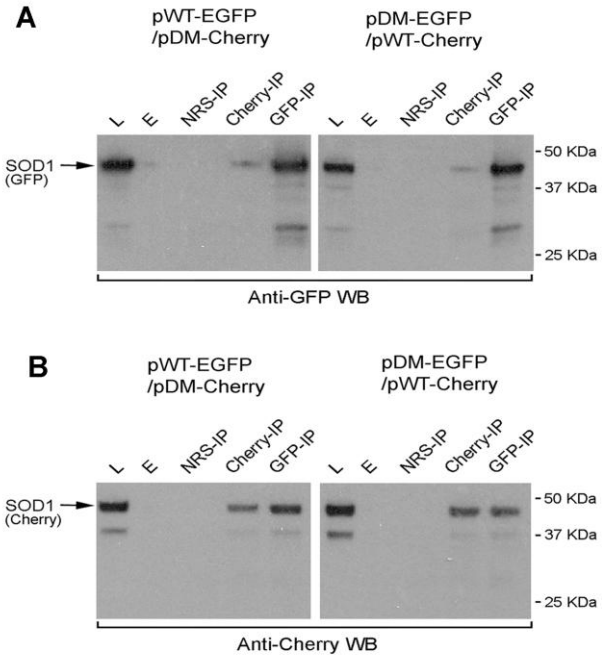
A
pWT-EGFP
/pDM-Cherry
pDM-EGFP
/pWT-Cherry
L
E
NRS-IP
Cherry-IP
GFP-IP
SOD1
(GFP)
50 KDa
37 KDa
25 KDa
Anti-GFP WB
B
pWT-EGFP
/pDM-Cherry
pDM-EGFP
/pWT-Cherry
SOD1
(Cherry)
Anti-Cherry WB